

A New Type of Quantum Criticality in the Pyrochlore Iridates

Lucile Savary,¹ Eun-Gook Moon,¹ and Leon Balents²

¹*Department of Physics, University of California, Santa Barbara, CA 93106-9530, U.S.A.*

²*Kavli Institute for Theoretical Physics, University of California, Santa Barbara, CA 93106-4030, U.S.A.*

(Dated: February 4, 2014)

Magnetic fluctuations and electrons couple in intriguing ways in the vicinity of zero temperature phase transitions – quantum critical points – in conducting materials. Quantum criticality is implicated in non-Fermi liquid behavior of diverse materials, and in the formation of unconventional superconductors. Here we uncover an entirely new type of quantum critical point describing the onset of antiferromagnetism in a nodal semimetal engendered by the combination of strong spin-orbit coupling and electron correlations, and which is predicted to occur in the iridium oxide pyrochlores. We formulate and solve a field theory for this quantum critical point by renormalization group techniques, show that electrons and antiferromagnetic fluctuations are strongly coupled, and that both these excitations are modified in an essential way. This quantum critical point has many novel features, including strong emergent spatial anisotropy, a vital role for Coulomb interactions, and highly unconventional critical exponents. Our theory motivates and informs experiments on pyrochlore iridates, and constitutes a singular realistic example of a non-trivial quantum critical point with gapless fermions in three dimensions.

Antiferromagnetic quantum critical points (QCPs) are controlled by the interactions between electrons and magnetic fluctuations [1, 2]. In three dimensional metals with a Fermi surface, it is believed to be sufficient to consider Landau damping of the magnetic order parameter in a purely order parameter theory, which leads, following Hertz [3, 4], to mean field behavior. In two dimensions, the electronic Fermi surface and order parameter are strongly coupled, a fact which may be related to high-temperature superconductivity and associated phenomena. This problem is highly non-trivial and still an active research topic [5–8].

In this paper, we uncover a new antiferromagnetic QCP which is strongly coupled in *three* dimensions, engendered by spin-orbit coupled electronic structure. We consider a quadratic band-touching at the Fermi energy, as in the inverted band gap material HgTe, but having in mind the strongly correlated family of iridium oxide pyrochlores [9–12]. The latter have chemical formula $A_2\text{Ir}_2\text{O}_7$, and an antiferromagnetic phase transition indeed occurs both as a function of temperature and at zero temperature with varying chemical pressure (ionic radius of A) [13]. We show that the replacement of the Fermi surface by a point Fermi node alters the physics in an essential way, suppressing screening of the Coulomb interaction and allowing the order-parameter fluctuations to affect *all* the low-energy electrons. These two facts lead to a strongly-coupled quantum critical point.

The nodal nature of the Fermi point, happily, also enables a rather complete analysis of the problem, which we present here, using the powerful renormalization group (RG) technique. The complete theory we present is in sharp contrast to the strongly coupled Fermi surface problem in two dimensions, which remains only partially understood and controversial. Finally, the pyrochlore quantum critical point has a remarkable symmetry structure. We find that, unlike at most classical and quantum phase transitions, rotational invariance is strongly broken

in the critical theory: the fixed point “remembers” the cubic anisotropy of space (and indeed takes it to an extreme limit, as explained further below). Compensating for the absence of spatial rotational invariance is, however, an *emergent* $SO(3)$ invariance of the critical field theory, which is a purely internal symmetry and unrelated to spatial rotations. The *anisotropy* in real space manifests for example in the formation of “spiky” Fermi surfaces when the system close to the QCP is doped with charge carriers, as seen in Fig. 1.

To proceed with the analysis, we couple the electrons to an Ising magnetic order parameter ϕ . This corresponds for the pyrochlore iridates to the translationally-invariant “all-in-all-out” (AIAO) antiferromagnetic state (see “inset” in Fig. 1), for which there is considerable evidence [14–16]. Due to the time-reversal and inversion symmetries of the paramagnetic state, electron bands are two-fold degenerate, so that band touching necessitates a minimal four-band model. Therefore the Hamiltonian is expressed in terms of four-component fermion operators ψ, ψ^\dagger , in addition to ϕ and the electrostatic field φ , which mediates the Coulomb interactions. The action is

$$\mathcal{S} = \int d^3x d\tau \psi^\dagger (\alpha \partial_\tau + \mathcal{H}_0(-i\nabla) + ie\varphi + gM\phi) \psi + \int d^3x d\tau \frac{1}{2} [(\nabla\varphi)^2 + (\nabla\phi)^2 + (\partial_\tau\phi)^2 + r\phi^2], \quad (1)$$

where the momentum cutoff (Λ) is assumed, and where the Hamiltonian density is $\mathcal{H}_0(\mathbf{k}) = c_0\mathbf{k}^2 + \sum_{a=1}^5 \hat{c}_a d_a(\mathbf{k}) \Gamma_a$. Higher-order terms omitted in Eq. (1) prove irrelevant at the QCP. The d_a ’s (given in the Supp. Mat. [17]) make a complete basis of the allowed terms quadratic in k_j , chosen such that $d_{1,2,3}$ belong to a three-dimensional representation (often called T_{2g}) and $d_{4,5}$ make a two-dimensional one (commonly referred to as E_g), the Γ_a ’s are anticommuting unit matrices, $\{\Gamma_a, \Gamma_b\} = 2\delta_{ab}$, $\Gamma_{ab} = \frac{-i}{2}[\Gamma_a, \Gamma_b]$, $\hat{c}_1 = \hat{c}_2 = \hat{c}_3 = c_1$ and $\hat{c}_4 = \hat{c}_5 = c_2$ (as they should since they belong to the

same representation), and symmetry dictates [17] the order parameter couples via the matrix $M = \Gamma_{45}$ ($\in A_{2g}$). e is the magnitude of the electron charge, and $g \in \mathbf{R}$ parametrizes the coupling strength of the fermions to the order parameter. As discussed in the Supplementary Material [17], $c_{0,1,2}$ may always be chosen positive, without loss of generality. c_0 parametrizes “particle-hole asymmetry”, with $c_0 = 0$ denoting a symmetric band structure. Also, when $c_0 \leq c_1/\sqrt{6}$, in the vicinity of the Gamma point, the bands touch at and only at the Gamma point. We assume that the system parameters fall within this range, and find that this is consistent.

The model in Eq. (1) has two phases. For $r > r_c \sim g^2$ (where r_c is thereby defined), ϕ fluctuates around zero, and can be integrated out. This is a magnetically disordered state. The resulting model with Coulomb interactions alone describes a non-Fermi liquid *phase*, as first discussed by Abrikosov and Beneslavskii [18, 19] and thoroughly revisited recently [10]. Notably, in this regime, non-trivial scaling exponents arise and the low-energy electronic dispersion renormalizes to become *isotropic*, i.e. effectively $c_1 \rightarrow c_2$ and $c_0 \ll c_1$. For $r < r_c$, the expectation value $\langle \phi \rangle \neq 0$, and replacing $\phi \rightarrow \langle \phi \rangle$ causes the two-fold degenerate bands to split, removing the quadratic touching at $\mathbf{k} = \mathbf{0}$ in favor of eight linearly-dispersing “Weyl points” along the $\langle 111 \rangle$ directions: a *Weyl semimetal*.

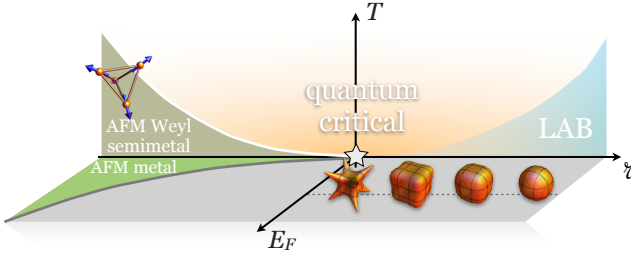


FIG. 1. Quantum critical point (QCP) and quantum criticality driven by the onset of “all-in-all-out” magnetism. For $r \geq r_c$ (in this figure the star indicates r_c), the “Luttinger-Abrikosov-Beneslavskii” (LAB) phase occurs at $T = 0$, with a quadratic Fermi node, while antiferromagnetic (AFM) “all-in-all-out” ordering occurs for $r < r_c$, with the quadratic node replaced by linear Weyl points – a Weyl semimetal. The quantum critical regime occurs at $T > 0$ around $r = r_c$. Note that the quantum critical-AFM boundary (thick white line) is a true (continuous Ising) phase transition. The E_F axis represents the Fermi energy and parametrizes electron or hole doping. The three-dimensional (orange) surfaces represent the shapes of the corresponding Fermi surfaces at small doping – the increased anisotropy is apparent as one moves towards the QCP. The phase transition denoted by the thick gray line is expected to exhibit critical properties appropriate to a $\mathbf{q} = \mathbf{0}$ order parameter coupled to a Fermi surface, as in the Hertz formulation [3], though subject to the usual uncertainties regarding the theory of that problem [5–7].

We now turn to the critical regime. To proceed, we introduce as a formal device N copies of the four fermion

fields, replacing $g \rightarrow g/\sqrt{N}$ (resp. $ie \rightarrow ie/\sqrt{N}$) and $\Gamma_a \rightarrow \Gamma_a \otimes 1_N$ (1_N is the $N \times N$ identity matrix). We organize perturbation theory in powers of $1/N$, but in the end argue that the results are asymptotically exact for the physical case $N = 1$. To leading order in $1/N$, we require the two boson self-energies in Fig. 2, and, using the dressed boson propagators including this correction, the fermion self-energy and vertex functions in Fig. 3. These diagrams allow a full calculation of the $O(1/N)$ terms of all critical exponents. The evaluation of the diagrams is complicated by the three mass parameters of the free fermion propagators. Fortunately, a simplification is possible due to the structure of the RG. While the (inverse) mass terms c_0 , c_1 , and c_2 all have identical engineering dimensions, they, in general renormalize differently from loop corrections, and thus their ratios *flow* in the full RG treatment. We find below that, in the critical regime, $c_0/c_2, c_1/c_2 \rightarrow 0$ under renormalization (arguments why this is the only reasonable choice are given in the Supplementary Material [17]). This allows technical simplifications in the loop integrals, and also has physical consequences we explore later.

In particular, in the limit $c_1/c_2 \rightarrow 0$, the interband splitting vanishes along the $\langle 111 \rangle$ directions, leading to an extended singularity of the electron Green’s function. In the loop integrals determining the bosonic self-energies, this produces a divergent contribution at non-zero \mathbf{k} . Technically, with the assumptions $c_0/c_2, c_1/c_2 \ll 1$ and $c_0/c_1 < 1/\sqrt{6}$ (shown self-consistent below), the low-energy behavior (small ω_n, \mathbf{k}) may be extracted as (see Supplementary Material [17])

$$\Sigma_b(\omega_n, \mathbf{k}) = -r_b^c + \frac{g_b^2}{\alpha} \left(|\ln c_1/c_2| |\mathbf{k}| f_b(\hat{\mathbf{k}}) + \sqrt{|\omega_n|} C_b \right), \quad (2)$$

where $r_\phi^c = r_c \sim g^2 \Lambda$, where Λ is an upper momentum cutoff, $g_\phi = g$, $g_\varphi = ie$, and $r_\varphi^c = C_\varphi = 0$ follows from charge conservation. $C_\phi \approx 1.33$ and the functions $f_b(\hat{\mathbf{k}})$ are given as integrals in the Supplementary Material [17].

Note that, at low energy, the dispersive terms in Eq. (2) are much larger than the bare \mathbf{k}^2, ω_n^2 terms they correct, and hence dominate the renormalized Green’s functions. Thus, in the fermion self-energy and vertex correction, the renormalized boson propagator, $\mathcal{G}_b^{-1} = \mathcal{G}_{b,0}^{-1} + \Sigma_b \approx \Sigma_b + r_b$ (note $r_\varphi = 0$), must be used. This renormalized boson propagator corresponds to the $N = \infty$ result, and already reveals some dramatic features. First, the bosons immediately receive a large anomalous scaling dimension, equal to 1, and their dynamics becomes damping-dominated, with dynamical critical exponents close to 2. Second, since the damping terms which dominate \mathcal{G}_b^{-1} are proportional to g_b^2 , it implies that the fermion self-energies, which involve two interaction vertices (see Fig. 3), become g_b independent: this is a sign of universality at the QCP.

To confirm the assumed scaling of $c_1/c_2, c_0/c_2$, and fully determine the critical behavior, we turn to the renormalization group approach. There, as usual, we ap-

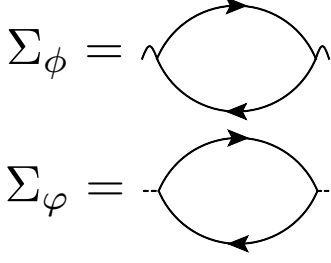


FIG. 2. Boson self energies for the order parameter (Σ_ϕ) and electrostatic (Σ_φ) fields.

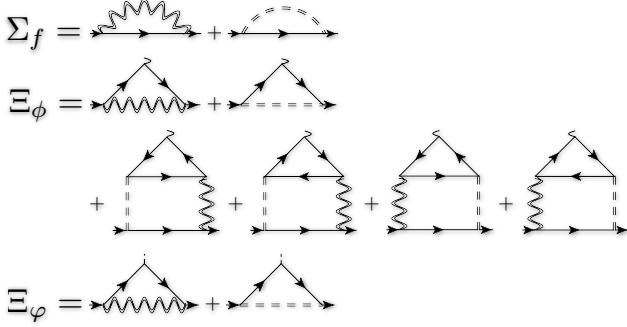


FIG. 3. $1/N$ diagrams for the fermion self-energy Σ_f and vertex corrections Ξ_ϕ and Ξ_φ (only two-loop diagrams that need be calculated, i.e. that do not vanish or cancel one another, are shown). Double lines indicate the renormalized boson propagators including the self-energies from Fig. 2. Expressions for these diagrams are given in the Supplementary Material [17].

ply the following rescaling (applicable in real space)

$$\begin{aligned} x &\rightarrow e^\ell x, \quad \tau \rightarrow e^{\int_0^\ell d\ell' z(\ell')} \tau, \quad \psi \rightarrow e^{-\int_0^\ell d\ell' \Delta_\psi(\ell')} \psi, \\ \phi &\rightarrow e^{-\int_0^\ell d\ell' \Delta_\phi(\ell')} \phi, \quad \varphi \rightarrow e^{-\int_0^\ell d\ell' \Delta_\varphi(\ell')} \varphi, \end{aligned} \quad (3)$$

where $\ell \geq 0$ parametrizes the RG flow. The exponents are left allowed to be scale dependent, as is necessary [20], as we shall see below.

We evaluate the contributions to the fermion propagator and coupling constants due to a small change in the cutoff (which corresponds physically to integrating out modes to keep the rescaled cutoff unchanged). Hence, the RG flow equations are obtained by (i) logarithmically differentiating the fermion self energy and vertex functions with respect to the cutoff Λ (made soft through a rapidly decaying function $|\mathbf{q}|/\Lambda \mapsto \mathcal{F}(|\mathbf{q}|/\Lambda)$) [20, 21], and (ii) identifying the appropriate coefficients of the Taylor expansion (in k_i and ω_n) of the result [22].

We leave most details to the Supplementary Material [17], and only give one example here. To extract the correction to the mass coefficient c_1 , we first expand the fermion self-energy as

$$\Sigma_f(\omega_n, \mathbf{k}) = \Sigma_f^0 I + \sum_{a=1}^5 \Sigma_f^a \Gamma_a, \quad (4)$$

and examine the Σ_f^1 component. The RG equation is then

$$\frac{\partial_\ell c_1}{c_1} = z + 1 - 2\Delta_\psi + \frac{\sqrt{2}}{c_1} \left(\partial_{k_x, k_y}^2 \left[\Lambda \frac{d}{d\Lambda} \Sigma_f^1 \right] \right) \Big|_{\omega_n=0, \mathbf{k}=0} \quad (5)$$

(we define $d_1(\mathbf{k}) = k_x k_y / \sqrt{2}$ [17]). Similar expressions are obtained for the other parameters of the theory, c_0 , c_2 , α , g and ie . The latter all depend on c_1 and c_2 through $1/(N |\ln c_1/c_2|)$ or $1/(N |\ln c_1/c_2|^2)$ (expressions are expanded in small $1/|\ln c_1/c_2|$, see Supp. Mat. [17]). Therefore, for the six equations thereby obtained, there are four unknowns (z , Δ_ψ , Δ_ϕ and Δ_φ) which can be chosen to keep four parameter fixed, leaving two left to flow. Here we find it is possible to keep α , g , (ie) and c_2 fixed, and thus c_1/c_2 and c_0/c_2 will flow. Note that, in doing so, we obtain a critical theory with non-zero coupling of fermions both to order-parameter and Coulomb-potential fluctuations: both effects are crucial and important in stabilizing the QCP. Finally, we obtain

$$z(\ell) = 2 - \delta z(\ell), \quad \Delta_\psi(\ell) = \frac{3 + \eta_\psi(\ell)}{2}, \quad \Delta_b(\ell) = \frac{3 + \eta_b(\ell)}{2}, \quad (6)$$

where $\delta z = \frac{0.0634}{|\ln c_1/c_2| N}$, $\eta_\psi = \frac{0.287}{|\ln c_1/c_2|^2 N}$, $\eta_\phi = 1 + \frac{0.510}{|\ln c_1/c_2| N}$ and $\eta_\varphi = 1 - \frac{0.127}{|\ln c_1/c_2| N}$.

The flow equations may be solved thanks to that of c_1/c_2 , which is an analytically-soluble differential equation involving only c_1/c_2 [17]. Ultimately, we find

$$(c_1/c_2)(\ell) = e^{-\frac{v_0}{\sqrt{N}} \sqrt{\ell + \ell_0}}, \quad \text{and} \quad (c_0/c_1)(\ell) = \Upsilon_0 e^{-\frac{v'_0}{\sqrt{N}} \sqrt{\ell + \ell_0}}, \quad (7)$$

with $v_0 = 0.202$, $v'_0 = 0.424$ and where ℓ_0 and Υ_0 are constants which depend on the system's parameters, namely on $c_{0,1,2}(\ell = 0)$. Formally, therefore both the c_0 and c_1 mass terms are irrelevant in the RG sense, but they can be “dangerously irrelevant” insofar as they control certain physical properties (see below). Note also that not only is c_0 irrelevant, but it also flows to zero *faster* than c_1 , so that c_0/c_1 becomes small at the QCP.

Intuition for the irrelevance of c_1 comes from considering the fermion self-energy Σ_f , which yields the corrections to $c_{0,1,2}$ and to α , and is given *schematically* by $\Sigma_f = \mathcal{G}_\phi M G_0 M + \mathcal{G}_\varphi G_0$ (the contributions from each boson field just add up). In the first term, which represents dressing of electrons by magnetic fluctuations, the appearance of M , which commutes with $\Gamma_{1,2,3}$ but *anti*-commutes with $\Gamma_{4,5}$, portends “opposite” consequences for c_1 and c_2 . The second term, due to Coulomb effects, tends instead to affect c_1 and c_2 identically. Our calculation shows that the former tendency prevails, and $c_1/c_2 \rightarrow 0$ under RG, as claimed above. Conversely, the fact that $c_0/c_1 \rightarrow_{\ell \rightarrow \infty} 0$ should be attributed to the effect of Coulomb forces, which suppress particle-hole asymmetry. Indeed, we have checked that if in the calculations we artificially turn off the long-range Coulomb potential, i.e. take $e = 0$, the QCP is unstable and there is no direct, continuous quantum phase transition from the LAB state to the AIAO one [17].

Eqs. (6,7) determine the properties at the QCP. We now turn to a discussion of the physical consequences. First we consider some scaling properties. For the correlation length, we need the flow equation for $\delta r = r - r_c$, the deviation from the critical point: $\partial_\ell(\delta r) = \nu^{-1}(\delta r)$, with $\nu = 1/[2 - \eta_\phi(\ell) - \delta z(\ell)]$. This implies, in the usual way, that the correlation length behaves as $\xi \sim (\delta r)^{-\nu}$, up to logarithmic corrections. Also interesting is the order parameter growth in the AIAO phase. By scaling, $\langle \phi \rangle \sim \xi^{-\Delta_\phi} \sim |\delta r|^\beta$, with $\beta = \Delta_\phi \nu$. We also expect the critical temperature of the magnetic state to obey $T_c \sim \xi^{-z} \sim |\delta r|^{z\nu}$. In asymptopia, i.e. $\ell \rightarrow \infty$, all the N -dependent corrections vanish, and the exponents correspond to those of a saddle-point treatment of φ, ϕ . These are still distinct from the usual order parameter mean field theory, as witnessed by the large ($\eta_\phi^\infty = \eta_\varphi^\infty = 1$) anomalous dimensions in this limit, and the unconventional values $\nu^\infty = 1$, $\beta^\infty = (z\nu)^\infty = 2$. The latter is noteworthy insofar as it implies an unusually wide critical fan at $T > 0$ which is controlled by the QCP (see Fig. 1). The RG treatment goes beyond the saddle point in giving the corrections due to finite c_1/c_2 , which are small only logarithmically, and thus may be significant for physically-realistic situations. For example we find $\langle \phi \rangle \sim (\delta r)^2 \exp\left[\frac{13.9}{\sqrt{N}} \sqrt{\ln \frac{\delta r}{r_0}}\right]$ [17], where r_0 is a constant.

The irrelevance of c_0 and c_1 has other, more direct, physical consequences. Because of the former, the low-energy electronic spectrum becomes approximately particle-hole symmetric. The latter has more implications. Obviously, the electronic spectrum develops pronounced cubic anisotropy, with anomalously low energy excitations along the cubic $\langle 111 \rangle$ directions in momentum space. This is in stark contrast to most critical points (for example of Ginzburg-Landau type, or involving Dirac fermions), which typically have emergent spatial isotropy and even conformal symmetry and Lorentz invariance at the fixed point. These low-energy excitations manifest, for example, in the specific heat c_v . Since at the Gaussian level the coefficient of $T^{3/2}$ diverges as $c_1^{-3/2}$, we estimate, by using $\ell \sim \frac{1}{z} \ln T_0/T$ as a cut-off (T_0 is a microscopic energy scale), $c_v \sim \exp\left[\frac{3v_0}{2\sqrt{N}\sqrt{z}} \sqrt{\ln \frac{T_0}{T}}\right] T^{3/2}$, with $z \approx 2$ [17]. The emergent anisotropy may also manifest in increasingly-“spiky” Fermi surfaces in lightly doped samples near the QCP, see Fig. 1.

Although rotational symmetry is strongly broken, the vanishing of c_1 leads to an *emergent internal* $SO(3)$ symmetry, corresponding to rotating the Γ_a matrices with $a = 1, 2, 3$ amongst themselves like a vector. The generator of this symmetry is the $SU(2)$ pseudo-spin \mathbf{I} , with

$$I_a = -\frac{1}{4}\epsilon_{abc}\psi^\dagger\Gamma_{bc}\psi = \psi^\dagger\left(-\frac{7}{6}J_a + \frac{2}{3}J_a^3\right)\psi, \quad (8)$$

where $a = x, y, z = 1, 2, 3$. Its integral has $SU(2)$ commutation relations and commutes with the fixed-point Hamiltonian.

Discussion.— In standard Hertz-Millis theory [3, 4],

the inequality $d + z > 4$ implies that the theory is above its critical dimension, and thus has mean field behavior. Although this inequality holds here, taking $z = 2$, the conclusion is false. The Hertz-Millis approach assumes the fermions may be innocuously integrated out, and obtains this inequality by power-counting the ϕ^4 term in the Landau action, which is irrelevant. Instead, here we have strong coupling of fermions with the order parameter, and the coupling term $\sim \phi\psi^\dagger\psi$ is *marginal* using $z = 2$, $\Delta_\phi = 2$, $\Delta_\psi = 3/2$. If one *does* integrate out the fermions, one obtains a nonanalytic $|\phi|^{5/2}$ term [17], which overwhelms the naïve ϕ^4 one, and is again marginal by power counting. This $|\phi|^{5/2}$ dependence was obtained previously in Ref. [23], in the context of a mean-field treatment of related transitions. Note, however, that such a mean-field analysis integrating out fermions is not justified and misses important physics.

Our critical theory has some formal similarity to the theory of a two-dimensional nodal nematic QCP in a d -wave superconductor [20], insofar as both theories display “infinite anisotropy”: in our case due to $c_1/c_2 \rightarrow 0$ under RG. This suggests that, as in Ref. [20], at low energy *the perturbative expansion parameter is small for all N* , and that therefore our results apply directly at low energy to the physical case $N = 1$. This conclusion is appealing, though we have not shown it rigorously.

With the above results in hand, we comment on the connection to experiments. In the pyrochlore iridates, the QCP might be tuned by alloying the A-site atoms, e.g. $\text{Pr}_{2-2x}\text{Y}_{2x}\text{Ir}_2\text{O}_7$, or by pressurizing stoichiometric compounds nearby. The theory developed here, which relies only on cubic symmetry and strong SOC, may apply to other materials if the bands at the Fermi energy belong to the appropriate irreducible representation, and it would be interesting to search for other examples. Experimentally, the heavily-damped paramagnon could be observed in inelastic neutron or x-ray scattering. An explicit calculation of the fermion spectral function measured in angle resolved photoemission has been made neither here nor for the non-Fermi liquid paramagnetic state [10], and is an important problem for future theory. However, in general, the weak logarithmic flow of the Hamiltonian parameters signifies large self-energy corrections, and behavior somewhat similar to marginal Fermi-liquid theory may be expected.

We also mention some possible complications in the iridates. Impurity scattering is a relevant perturbation and hence important at low energy close to the band touching. Therefore, our results will apply best in the cleanest samples. Also, an accidental band crossing may occur away from the zone center, thereby shifting the Fermi level a few meV away from the nodal point. This should be addressed by *ab initio* calculations and experiments. In such a case, our results still hold for energies and/or temperatures above this shift energy. Finally, in many of the pyrochlore iridates, the A-site ion hosts rare-earth moments, which were not included here. They only weakly couple to the Ir electrons and to themselves, so are only

important at low energy. On the antiferromagnetic side of the QCP, the Ir spins act as strong local effective magnetic fields, locking the A-site spins. However, when the Ir sites are not ordered, as in $\text{Pr}_2\text{Ir}_2\text{O}_7$, A-site ions will have an effect below a few Kelvins. Several authors have proposed scenarios based on RKKY interactions [24–26], but the quantum critical theory expounded here should be an apt starting point for a systematic analysis.

Acknowledgements.— We thank Cenke Xu and Yong-

Baek Kim for discussions on prior work, Max Metlitski for pointing Ref. [20] to us, and acknowledge Ru Chen, Satoru Nakatsuji and Takeshi Kondo for sharing unpublished data. The integrals were performed using the Cuba library [27], and the Feynman diagrams in Figs. 2 and 3 drawn with JaxoDraw [28]. L.S. and L.B. were supported by the DOE through grant DE-FG02-08ER46524, and E.-G. M. was supported by the MRSEC Program of the National Science Foundation under Award No. DMR 1121053.

-
- [1] S. Sachdev, *Quantum Phase Transitions* (Cambridge University Press, Cambridge, 2011).
 - [2] H. v. Löhneysen, A. Rosch, M. Vojta, and P. Wölfle, *Rev. Mod. Phys.*, **79**, 1015 (2007).
 - [3] J. A. Hertz, *Phys. Rev. B*, **14**, 1165 (1976).
 - [4] A. J. Millis, *Phys. Rev. B*, **48**, 7183 (1993).
 - [5] S.-S. Lee, *Phys. Rev. B*, **80**, 165102 (2009).
 - [6] M. A. Metlitski and S. Sachdev, *Phys. Rev. B*, **82**, 075128 (2010).
 - [7] D. F. Mross, J. McGreevy, H. Liu, and T. Senthil, *Phys. Rev. B*, **82**, 045121 (2010).
 - [8] K. Efetov, H. Meier, and C. Pépin, *Nature Physics*, **9**, 442 (2013).
 - [9] X. Wan, A. M. Turner, A. Vishwanath, and S. Y. Savrasov, *Phys. Rev. B*, **83**, 205101 (2011).
 - [10] E.-G. Moon, C. Xu, Y. B. Kim, and L. Balents, *Phys. Rev. Lett.*, **111**, 206401 (2013).
 - [11] R. Chen, E.-G. Moon, and L. Balents, unpublished (2014).
 - [12] T. Kondo, S. Nakatsuji, *et al.*, private communication (2014).
 - [13] K. Matsuhira, M. Wakeshima, Y. Hinatsu, and S. Takagi, *Journal of the Physical Society of Japan*, **80**, 094701 (2011).
 - [14] H. Sagayama, D. Uematsu, T. Arima, K. Sugimoto, J. J. Ishikawa, E. O’Farrell, and S. Nakatsuji, *Phys. Rev. B*, **87**, 100403 (2013).
 - [15] K. Tomiyasu, K. Matsuhira, K. Iwasa, M. Watahiki, S. Takagi, M. Wakeshima, Y. Hinatsu, M. Yokoyama, K. Ohoyama, and K. Yamada, *J. Phys. Soc. Jpn*, **81**, 034709 (2012).
 - [16] S. M. Disseler, C. Dhital, A. Amato, S. R. Giblin, C. de la Cruz, S. D. Wilson, and M. J. Graf, *Phys. Rev. B*, **86**, 014428 (2012).
 - [17] See Supplementary Material for details of definitions and calculations not given in the main text.
 - [18] A. A. Abrikosov and S. D. Beneslavskii, *Sov. Phys. JETP*, **32**, 699 (1971).
 - [19] A. A. Abrikosov, *Sov. Phys. JETP*, **39**, 709 (1974).
 - [20] Y. Huh and S. Sachdev, *Phys. Rev. B*, **78**, 064512 (2008).
 - [21] M. Vojta, Y. Zhang, and S. Sachdev, *Int. J. Mod. Phys. B*, **14**, 3719 (2000).
 - [22] Note that a number of technicalities are involved in this calculation, in particular regarding the convergence of the differentiated functions; All are discussed in the Supplementary Material [17].
 - [23] M. Kurita, Y. Yamaji, and M. Imada, *Phys. Rev. B*, **88**, 115143 (2013).
 - [24] G. Chen and M. Hermele, *Phys. Rev. B*, **86**, 235129 (2012).
 - [25] R. Flint and T. Senthil, *Phys. Rev. B*, **87**, 125147 (2013).
 - [26] S. Lee, A. Paramekanti, and Y. B. Kim, *Phys. Rev. Lett.*, **111**, 196601 (2013).
 - [27] T. Hahn, *Computer Physics Communications*, **168**, 78 (2005), ISSN 0010-4655.
 - [28] D. Binosi and L. Theul, *Computer Physics Communications*, **161**, 76 (2004), ISSN 0010-4655.
 - [29] J. M. Luttinger, *Phys. Rev.*, **102**, 1030 (1956).
 - [30] S. Murakami, N. Nagaosa, and S.-C. Zhang, *Phys. Rev. B*, **69**, 235206 (2004).
 - [31] M. Kardar, *Statistical Physics of Fields* (Cambridge University Press, Cambridge, 2007).
-

SUPPLEMENTARY MATERIAL

In reciprocal space, the action, Eq. (1) in the main text, is

$$\begin{aligned}
 S = & \int_{-\infty}^{\infty} \frac{d\omega_n}{2\pi} \int_{\Lambda} \frac{d^3k}{(2\pi)^3} \left[\phi_{-\omega_n, -\mathbf{k}} \left(\frac{\omega_n^2}{2} + \frac{\mathbf{k}^2}{2} + \frac{r}{2} \right) \phi_{\omega_n, \mathbf{k}} + \varphi_{-\omega_n, -\mathbf{k}} \left(\frac{\mathbf{k}^2}{2} \right) \varphi_{\omega_n, \mathbf{k}} \right. \\
 & + \psi_{\omega_n, \mathbf{k}}^{\dagger} \left(-\alpha i\omega_n + c_0 \mathbf{k}^2 + \sum_{a=1}^5 \hat{c}_a d_a(\mathbf{k}) \Gamma_a \right) \psi_{\omega_n, \mathbf{k}} \\
 & \left. + g \int_{-\infty}^{\infty} \frac{d\omega'_n}{2\pi} \int_{\Lambda} \frac{d^3k'}{(2\pi)^3} \phi_{\omega'_n - \omega_n, \mathbf{k}' - \mathbf{k}} \psi_{\omega'_n, \mathbf{k}'}^{\dagger} M \psi_{\omega_n, \mathbf{k}} + ie \int_{-\infty}^{\infty} \frac{d\omega'_n}{2\pi} \int_{\Lambda} \frac{d^3k'}{(2\pi)^3} \varphi_{\omega'_n - \omega_n, \mathbf{k}' - \mathbf{k}} \psi_{\omega'_n, \mathbf{k}'}^{\dagger} \psi_{\omega_n, \mathbf{k}} \right], \quad (9)
 \end{aligned}$$

where all the notations are defined in Sec. I of the present

Supplementary Material. Throughout the latter, for ease

of presentation, we shift the QCP so that $r_c = 0$.

I. NOTATIONS AND SYMMETRIES

In this section, we provide more information about the notations used in the main text and a more detailed discussion of the symmetries at play.

A. Fermion Hamiltonian

The fermionic Hamiltonian density in the disordered (quadratic band touching) phase reads

$$\begin{aligned}\mathcal{H}_0(\mathbf{k}) &= \alpha_1 \mathbf{k}^2 + \alpha_2 (\mathbf{k} \cdot \mathbf{J})^2 + \alpha_3 (k_x^2 J_x^2 + k_y^2 J_y^2 + k_z^2 J_z^2) \\ &= c_0 \mathbf{k}^2 + \sum_{a=1}^5 \hat{c}_a d_a(\mathbf{k}) \Gamma_a,\end{aligned}\quad (10)$$

where $\hat{c}_1 = \hat{c}_2 = \hat{c}_3 = c_1$ and $\hat{c}_4 = \hat{c}_5 = c_2$. The first line uses the conventional Luttinger parameters ($\alpha_{1,2,3}$) in the $j = 3/2$ matrix representation [29], and the second line is the form used in the main text. The Gamma matrices (Γ_a) form a Clifford algebra, $\{\Gamma_a, \Gamma_b\} = 2\delta_{ab}$, and have been introduced as described in the literature [30]. Note that c_0 quantifies the particle-hole asymmetry, while $|c_1 - c_2|$ naturally characterizes the cubic anisotropy. The energy eigenvalues are $E_{\pm}(\mathbf{k}) = c_0 \mathbf{k}^2 \pm E(\mathbf{k})$, where

$$E(\mathbf{k}) = \sqrt{\sum_{a=1}^5 \hat{c}_a^2 d_a^2(\mathbf{k})}$$

$$\begin{aligned}d_1(\mathbf{k}) &= \frac{k_x k_y}{\sqrt{2}}, & d_2(\mathbf{k}) &= \frac{k_x k_z}{\sqrt{2}}, & d_3(\mathbf{k}) &= \frac{k_y k_z}{\sqrt{2}} \\ d_4(\mathbf{k}) &= \frac{k_x^2 - k_y^2}{2\sqrt{2}}, & d_5(\mathbf{k}) &= \frac{2k_z^2 - k_x^2 - k_y^2}{2\sqrt{6}}.\end{aligned}$$

It is very important to note that, in the limit $c_{0,1} \rightarrow 0$, $E(\mathbf{k})$ and the energy spectrum $E_{\pm}(\mathbf{k})$ become gapless along the $\langle 111 \rangle$ directions. When needed, a “regularization” is then possible, for example by introducing higher momentum dependence in $c_{1,2}$, e.g. $c_{1,2} \rightarrow c_{1,2} + \lambda \mathbf{k}^2$.

It is straightforward to relate the coefficients used in the main text to the Luttinger α_i parameters. This can be done by expressing the spin operators in terms of the Gamma matrices, using for example the equalities

$$\begin{aligned}J_x &= \frac{\sqrt{3}}{2} \Gamma_{15} - \frac{1}{2} (\Gamma_{23} - \Gamma_{14}), \\ J_y &= -\frac{\sqrt{3}}{2} \Gamma_{25} + \frac{1}{2} (\Gamma_{13} + \Gamma_{24}), \\ J_z &= -\Gamma_{34} - \frac{1}{2} \Gamma_{12},\end{aligned}\quad (11)$$

where $\Gamma_{ab} = \frac{1}{2i} [\Gamma_a, \Gamma_b]$.

The fermion bare Green’s function is

$$G_{\omega_n, \mathbf{k}}^0 = \frac{1}{-i\alpha\omega_n + \mathcal{H}_0(\mathbf{k})} = \frac{1}{-i\alpha\omega_n + E_{\epsilon}(\mathbf{k})} P_{\epsilon}(\mathbf{k}),$$

where the sum over $\epsilon = \pm 1$ is implicit and $P_{\epsilon}(\mathbf{k}) = \frac{1}{2} \left(1 + \epsilon \frac{\mathcal{H}_0(\mathbf{k}) - c_0 \mathbf{k}^2}{E(\mathbf{k})} \right)$ is a projection operator, $P_{\epsilon}^2(\mathbf{k}) = 1$.

B. Symmetries

It is useful to recap the symmetries of the system in the absence of all-in-all-out order, and detail the remaining symmetries in its presence.

As defined above and in Refs. [30] and [10], the Γ_a matrices are even under time-reversal and inversion symmetry, while the Γ_{ab} are even under inversion, but odd under time-reversal.

As is well-known for some semiconductors, like HgTe, the touching of four bands at the Gamma point is protected by cubic symmetries (the bands at the Gamma point belong to a four-dimensional representation of the cubic group O_h), and the absence of a linear term follows from time-reversal and cubic (inversion) symmetries. Moreover, thanks to inversion and time-reversal symmetries, all bands are doubly-degenerate away from the Gamma point.

The magnetic order parameter field ϕ transforms as follows under the symmetries of the “disordered” system. It is odd under time-reversal symmetry (since the spins $\vec{S} \rightarrow -\vec{S}$ under time-reversal), and so only the (time-reversal-odd) Γ_{ab} can couple to it. It is even under inversion (since $\vec{S} \rightarrow \vec{S}$ under inversion), unchanged under three-fold rotations, and odd under the allowed reflections of the pyrochlore lattice. A single Gamma matrix, namely $\Gamma_{45} \propto J_x J_y J_z + J_z J_y J_x$ [10, 30] (see below), transforms identically.

The Hamiltonian at *fixed* \mathbf{k} , i.e. $\mathcal{H}_0(\mathbf{k})$, together with the coupling to the order parameter with $\phi \neq 0$, which we call $\mathcal{H}_1(\mathbf{k})$, have the following transformation properties. For $\mathbf{k} \parallel \langle 111 \rangle$, \mathcal{H}_1 is invariant under three-fold rotations about \mathbf{k} , and reflections with respect to planes that contain \mathbf{k} . For $\mathbf{k} = \mathbf{0}$, there is additionally inversion symmetry. The symmetry group at $\mathbf{k} = \mathbf{0}$ then decomposes the four bands of interest into two two-dimensional representations. For $\mathbf{k} \neq \mathbf{0}$, symmetries do not impose bands to cross, hence making any crossings “accidental.” However, it is noteworthy that the purely quadratic Hamiltonian \mathcal{H}_0 we study, with $c_0 \leq c_1/\sqrt{6}$ and $c_1 \leq c_2/\sqrt{6}$, in the presence of the linear coupling to the order parameter $\phi \psi^\dagger \Gamma_{45} \psi$ leads inevitably to band crossings along the $\langle 111 \rangle$ directions.

Note that the system in the presence of an external applied magnetic field, discussed in Ref. [10], is less symmetric. The system’s Hamiltonian at fixed \mathbf{k} , which we call $\mathcal{H}_2(\mathbf{k})$, is only invariant under three-fold rotations about \mathbf{k} if both the magnetic field and \mathbf{k} point along the same $\langle 111 \rangle$ direction. For $\mathbf{k} = \mathbf{0}$ the system has additionally inversion symmetry, but all the representations of the symmetry group are one-dimensional anyway, and there is a priori no degeneracy at $\mathbf{k} = \mathbf{0}$. Away from $\mathbf{k} = \mathbf{0}$, any band crossing is, again, accidental.

It is important to note that, although no crossings are required by symmetry, once the crossings are found to happen, their properties are “stable” in the sense that (i) no symmetry-preserving perturbation will remove them, (ii) the dispersion along the crossings will remain linear,

(iii) they will not move away from the $\langle 111 \rangle$ axes.

C. Couplings

The long-range Coulomb interaction is described by introducing the Hubbard-Stratonovich field, φ , which couples to the density of fermions.

The all-in all-out operator is represented by the time-reversal symmetry breaking Ising field (ϕ) corresponding to $J_x J_y J_z + J_z J_y J_x$ in Luttinger's notation [29]. In terms of the Gamma matrices, the order parameter is $\Gamma_{45} \sim J_x J_y J_z + J_z J_y J_x$. Thus, finally, the interaction part of the action is the “vertex term” given, in real space and imaginary time, by

$$\mathcal{S}_{vertex} = \int d^3x d\tau \psi^\dagger [ie \varphi + g \phi \Gamma_{45}] \psi, \quad (12)$$

where ψ is the four-component spinor field. Upon extending the field space to N flavors of fermions, this term becomes

$$\mathcal{S}_{vertex} \rightarrow \frac{1}{\sqrt{N}} \int d^3x d\tau \psi^\dagger [ie \varphi + g \phi \Gamma_{45}] \psi. \quad (13)$$

By appropriately transforming the Gamma matrices with transformations not belonging to the cubic group, one may show that the signs of $c_{0,1,2}$ may always be taken positive. Therefore, throughout the paper we assume $c_{0,1,2} \geq 0$. We also assume $c_0 \leq c_1/\sqrt{6}$, i.e. we assume the two sets of bands have opposite curvatures in all directions at the Gamma point, or, in other words that the Fermi energy goes through the band touching point.

D. Green's function and self-energy conventions

We use the following conventions for the boson Green's functions, $\mathcal{G}_{b;\omega_n,\mathbf{k}}$ with $b = \phi, \varphi$, fermion Green's function, $G_{\omega_n,\mathbf{k}}$, boson self-energies, $\Sigma_b(\omega_n, \mathbf{k})$ and fermion self-energy, $\Sigma_f(\omega_n, \mathbf{k})$:

$$\begin{aligned} \mathcal{G}_{\varphi;\omega_n,\mathbf{k}} &= \langle \varphi_{-\mathbf{k}} \varphi_{\mathbf{k}} \rangle = \frac{1}{\mathbf{k}^2 + \Sigma_\varphi(\mathbf{k})}, \\ \mathcal{G}_{\phi;\omega_n,\mathbf{k}} &= \langle \phi_{-\omega_n, -\mathbf{k}} \phi_{\omega_n, \mathbf{k}} \rangle = \frac{1}{\mathbf{k}^2 + \omega_n^2 + r + \Sigma_\phi(\omega_n, \mathbf{k})}, \\ G_{\omega_n,\mathbf{k}}^{\mu\nu} &= \langle \psi_{\omega_n,\mathbf{k}}^\mu \psi_{\omega_n,\mathbf{k}}^{\nu\dagger} \rangle \\ &= [-i\alpha\omega_n + \mathcal{H}_0(\mathbf{k}) + \Sigma_f(\omega_n, \mathbf{k})]^{-1}, \end{aligned}$$

where $\mu, \nu = 1, \dots, 4$ (or $1, \dots, 4N$) but are omitted throughout. The “bare propagators” are denoted with the subscript or superscript “0.”

II. ASYMPTOTIC LIMITS OF THE BOSONIC SELF-ENERGIES

We first evaluate the boson self-energies in the large- N limit. They are given by

$$\Sigma_b(\omega_n, \mathbf{k}) = \frac{g_b^2}{N} \int_\Lambda \frac{d^3q}{(2\pi)^3} \int_{-\infty}^{+\infty} \frac{d\Omega_n}{2\pi} \text{Tr} [G_{\Omega_n, \mathbf{q}}^0 M_b G_{\Omega_n + \omega_n, \mathbf{q} + \mathbf{k}}^0 M_b], \quad (14)$$

where $g_\varphi = ie$, $g_\phi = g$, $M_\varphi = I$ and $M_\phi = \Gamma_{45}$ (I is the identity matrix). Here the subscript Λ in the q integral indicates that an ultraviolet cutoff is required to keep $\Sigma_b(0, \mathbf{0})$ finite. This determines the (non-universal) location of the QCP. However, we seek the corrections to this term for non-zero frequency and momenta, which are cutoff independent, and will be therefore obtained below without further discussion of Λ . We will return later to the role of the cutoff when considering fermionic self-energy terms, and treat it in more detail. The explicit expression for $\Sigma_b(\omega_n, \mathbf{k})$ at $c_0 \leq c_1/\sqrt{6}$ is

$$\Sigma_b(\omega_n, \mathbf{k}) = \frac{-g_b^2}{\alpha} \sum_{\epsilon=\pm} \int_\Lambda \frac{d^3q}{(2\pi)^3} \left[\frac{E_{\mathbf{q},\mathbf{k}}^+ + E_{\mathbf{q},\mathbf{k}}^- + \epsilon 2c_0 \mathbf{q} \cdot \mathbf{k}}{\alpha^2 \omega_n^2 + (E_{\mathbf{q},\mathbf{k}}^+ + E_{\mathbf{q},\mathbf{k}}^- + \epsilon 2c_0 \mathbf{q} \cdot \mathbf{k})^2} \right] \left(1 - \frac{F_{b;\mathbf{q},\mathbf{k}}}{E_{\mathbf{q},\mathbf{k}}^+ E_{\mathbf{q},\mathbf{k}}^-} \right),$$

where $E_{\mathbf{q},\mathbf{k}}^\pm = E(\mathbf{q} \pm \mathbf{k}/2)$ and $F_{b;\mathbf{q},\mathbf{k}} = \sum_{a=1}^5 (\varepsilon_a)^b \hat{c}_a^2 d_a(\mathbf{q} - \mathbf{k}/2) d_a(\mathbf{q} + \mathbf{k}/2)$, with $\varepsilon = (1 \ 1 \ 1 \ -1 \ -1)$ and $b = 0$ (resp. $b = 1$) for $b = \varphi$ (resp. $b = \phi$). Note that Σ_b is $O(1)$ (and not $O(1/N)$); mathematically this is because of the trace, which yields a factor of N .

As mentioned above, the boson self-energy $\Sigma_\phi(0, \mathbf{0})$ is finite but depends upon the cutoff ($\Sigma_\phi(0, \mathbf{0})$ is propor-

tional to Λ). Again, this determines the location of the QCP at $N = \infty$, and when we focus on the critical theory, this zero-frequency zero-momentum contribution is exactly cancelled by the bare value of r . Hence we are left with the corrections at non-zero frequency and momenta, which we isolate by considering the self-energy difference $\Sigma_b(\omega_n, \mathbf{k}) - \Sigma_b(0, \mathbf{0})$ (for $b = \varphi$ the second term is zero by charge conservation). This difference is finite and cutoff independent. In the $c_{0,1} \rightarrow 0$ limit, which will be the

case in the critical theory, the self-energy differences show logarithmic divergences, i.e. contain $|\ln c_1/c_2|$. Conveniently, as mentioned in the main text, the latter will act as a control parameter [20], in addition to N , in the critical theory.

In the following, we thereby obtain the one-loop bosonic self energy,

$$\begin{aligned} \Sigma_b(\omega_n, \mathbf{k}) - \Sigma_b(0, \mathbf{0}) \\ = \frac{g_b^2}{\alpha} \left(|\mathbf{k}| f_b(\hat{\mathbf{k}}) |\ln c_1/c_2| + \sqrt{|\omega_n|} C_b \right). \end{aligned} \quad (15)$$

For future convenience, we take henceforth $c_2 = 1$ and denote $c = c_1$. It is straightforward to obtain the coefficients of the frequency dependences, C_b . Because Σ_b is *larger* than the bare term at $r = 0$, which goes as $\mathbf{k}^2 + \omega_n^2$, throughout this work, we take $\mathcal{G}_b \rightarrow \Sigma_b^{-1}$, where \mathcal{G}_b is a full boson Green's function. Finally, note that we used an expansion in small $1/|\ln c_1/c_2|$ of Σ_b^{-1} , i.e. of the inverse of Eq. (15), in some of the calculations.

By evaluating $\Sigma_b(\omega_n, \mathbf{0}) - \Sigma_b(0, \mathbf{0})$, we find $C_\varphi = 0$ and $C_\phi = 1.33$ taking $\alpha = 1$, $c_1 = 0$ and $c_2 = 1$. Note that in the $c_1/c_2 \rightarrow 0$ limit, the frequency dependence is subdominant and the bosonic propagator becomes static.

We now extract the non-trivial logarithmic momentum dependence, $f_b(\hat{\mathbf{k}})$.

A. Coefficient of the logarithm

As mentioned above, when $c_{0,1} = 0$, to which the theory flows at the QCP, the energy $E(\mathbf{k})$ and spectrum $\mathbf{E}_\pm(\mathbf{k})$ vanish for any $\mathbf{k} \parallel \langle 111 \rangle$, which renders the self-energy difference, $\Sigma_b(\omega_n, \mathbf{k}) - \Sigma_b(0, \mathbf{0})$, *divergent*. The appearance of a divergence is subtle: for general \mathbf{k} , the denominator in Eq. (15) appears relatively well-behaved since the singularity occurs only when *both* $\mathbf{q} + \mathbf{k}/2$ and $\mathbf{q} - \mathbf{k}/2$ lie along a $\langle 111 \rangle$ axis. The singularity actually arises from the regions of integration at large $|\mathbf{q}|$ along these directions, where $|\mathbf{k}| \ll |\mathbf{q}|$, so that *both* energies are small. We analyze it below. In the limit $0 \leq c_0 \ll c_1 \ll c_2 = 1$ (i.e. with c_1 *nonzero* and small), which is the actual behavior in the RG *flows*, the divergence is removed, and the result is large in $|\ln c_1/c_2|$. In this subsection, we extract the leading result in this limit. Notably, in this limit, the result is independent of c_0 , and can be approximated by taking simply $c_0 = 0$.

To extract the coefficient of the logarithm, $f_b(\hat{\mathbf{k}})$, we rotate to bases whose x -axes point along one of the $\langle 111 \rangle$ directions, and make a change of variables such that

$$\begin{cases} \hat{\mathbf{e}}_1 = (s_1, s_2, s_3)/\sqrt{3} \\ \hat{\mathbf{e}}_2 = (0, s_2, -s_3)/\sqrt{2} \\ \hat{\mathbf{e}}_3 = (-2s_1, s_2, s_3)/\sqrt{6} \end{cases} \quad \text{and} \quad \mathbf{q} = \frac{Q}{c_1} \hat{\mathbf{e}}_1 + u \hat{\mathbf{e}}_2 + v \hat{\mathbf{e}}_3, \quad (16)$$

where $s_i = \pm 1$ (allows to span the eight $\langle 111 \rangle$ directions). This rewriting is chosen so that for Q, u, v of $O(1)$, the

region near the $(s_1 s_2 s_3)$ ray is singled out. The Jacobian of this coordinate transformation is $\mathcal{J}_0 = |s_1 s_2 s_3/c_1|$. Now, we rewrite the functions involved in the integrand of the self-energies, Eq. (15), in these new coordinates, and we obtain the leading asymptotic behavior of each such function at small c_1 .

For example, we find

$$E_{\mathbf{q}, \mathbf{k}}^\pm \approx \frac{1}{c_1} \epsilon_{Q,u,v;k_1,k_2,k_3}^\pm \quad \text{and} \quad F_{b;\mathbf{q}, \mathbf{k}} \approx \frac{1}{c_1^2} \gamma_{Q,u,v;k_1,k_2,k_3}^b, \quad (17)$$

where the ϵ_\pm and γ^b ($b = \varphi, \phi$) are functions of $\{Q, u, v, k_1, k_2, k_3\}$ (and of course of the s_i 's) *only*. We are then in a position to take the logarithmic derivatives of the boson self-energies. A major simplification thereby occurs: the frequency dependence drops out of $\Sigma_b(\omega_n, \mathbf{k}) - \Sigma_b(\omega_n, \mathbf{0})$. We find

$$\frac{\alpha}{g_b^2} c_1 \partial_{c_1} [\Sigma_b(\omega_n, \mathbf{k}) - \Sigma_b(\omega_n, \mathbf{0})] \quad (18)$$

$$\begin{aligned} &= \sum_{s_1, s_2, s_3 = \pm 1} \int_0^{+\infty} \frac{dQ}{2\pi} \int_{-\infty}^{+\infty} \frac{du}{2\pi} \int_{-\infty}^{+\infty} \frac{dv}{2\pi} \mathcal{K}_{s_1 s_2 s_3}^b \\ &= f_b(\mathbf{k}) = |\mathbf{k}| f_b(\hat{\mathbf{k}}), \end{aligned} \quad (19)$$

where

$$\begin{aligned} \mathcal{K}_{s_1, s_2, s_3}^b &= 9\sqrt{2} Q \left[\frac{3(a_0 - h_0^b)}{a_0^{5/2}} \right. \\ &\quad \left. + \frac{2(h^b(a_+ + \sqrt{a_+} \sqrt{a_-} + a_-) - 3a_+ a_-)}{a_+^2 a_+^{3/2} + a_+^2 a_-^{3/2}} \right]. \end{aligned} \quad (20)$$

In the above formula, we introduced several expressions:

$$\kappa = s_1 s_2 k_x k_y + s_1 s_3 k_x k_z + s_2 s_3 k_y k_z \quad (21)$$

$$h_0^\phi = 3 [Q^2 - 2(u^2 + v^2)] \quad (22)$$

$$a_0 = h_0^\varphi = 3 [Q^2 + 2(u^2 + v^2)] \quad (23)$$

$$h^\phi = h_0^\phi + (\mathbf{k}^2 - \kappa) \quad (24)$$

$$h^\varphi = h_0^\varphi - (\mathbf{k}^2 - \kappa) \quad (25)$$

$$\begin{aligned} a_\pm &= a_0 + \left(\mathbf{k}^2 - \kappa \pm 3\sqrt{2}u(s_2 k_y - s_3 k_z) \right. \\ &\quad \left. \pm \sqrt{6}v(s_2 k_y + s_3 k_z - 2s_1 k_x) \right), \end{aligned} \quad (26)$$

where all the functions defined above, namely h_0^b , a_0 , h^b , a_\pm , and \mathcal{K}^b ($b = \phi, \varphi$), are taken at $\{Q, u, v, k_x, k_y, k_z\}$ (and are also functions of the s_i 's although we have written the latter explicitly for \mathcal{K}^b only). Note that the integrations over u and v are taken all the way from $-\infty$ to $+\infty$ although the sum over the eight directions, \sum_{s_1, s_2, s_3} is also taken. This is because, for non-zero c_1 , the u, v integrations have a priori upper bounds of order Q/c_1 , which is taken to infinity. In the present order of limits, all contributions arise from regions of angular width of order c_1 from the $\langle 111 \rangle$ rays.

The integrals, Eq. (18), are evaluated thanks to the Cuba library, using the ‘‘Cuhre’’ routine [27].

B. Approximation

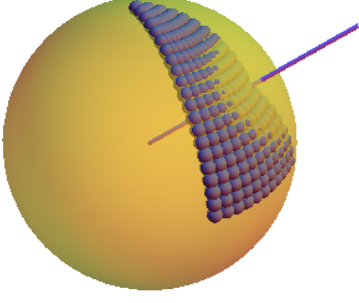


FIG. 4. Plot of $f_\phi(\mathbf{k})/f_\phi(001)$. The line represents a $\langle 111 \rangle$ direction. The whole surface can be obtained from the plotted points by applying cubic symmetries (note that the set of plotted points is larger than the minimal set of points). The yellow surface is a sphere of radius $f_\phi(001)$.

Since f_b is very smooth (see Fig. 4), we approximate it by a low-order polynomial of \mathbf{k} in order to be able to take accurate derivatives of f_b as required to compute the flow of c_1 (and c_2) – see Sec. III. Imposing cubic symmetry, the most general polynomial to order six can take the form

$$\frac{1}{f_b(\mathbf{k})} \approx m_1^b + m_2^b (\hat{k}_x^4 + \hat{k}_y^4 + \hat{k}_z^4) + m_3^b \hat{k}_x^2 \hat{k}_y^2 \hat{k}_z^2, \quad (27)$$

and fits with $m_1^\phi = 2.356$, $m_2^\phi = -0.130$ and $m_3^\phi = 4.136$ and $m_1^\varphi = -4.704$, $m_2^\varphi = 0.264$ and $m_3^\varphi = -8.253$ provide excellent approximations: the square roots of the means of the squares are $R_\phi = 0.0049$ and $R_\varphi = 0.0049$,

$$\text{where } R_b = \frac{1}{N_{\text{pts}}} \sqrt{\sum_{i=1}^{N_{\text{pts}}} \frac{((1/f_i^b) - \text{fit}_i^b)^2}{(1/f_i^b)^2}}.$$

III. RG EQUATIONS

As discussed in the main text, twenty-four Feynman diagrams are necessary to determine the RG equations: two boson self-energies, Σ_b , given in Sec. II, two fermion self-energies, $\Sigma_{f;b}$, and twenty vertex corrections, the one-loop $\Xi_{b;(1);b'}$ (four) and the two-loop $\Xi_{b;(2);b',b'',\eta}$ (sixteen, twelve of which either vanish identically or cancel out one another), with $b, b', b'' = \varphi, \phi$ and $\eta = \pm 1$. The

notation is expected to be transparent, and the expressions can be read off in Eqs. (28–30). We proceed like in Refs. [20, 21], i.e. we find the corrections to the parameters of the theory by evaluating the former when a small change in the cutoff is applied. It physically corresponds to integrating out modes to keep the rescaled cutoff unchanged. In practice, we (i) use soft momentum-cutoffs for the integrals, implemented by the use of a rapidly decaying function $|\mathbf{q}|/\Lambda \mapsto \mathcal{F}(|\mathbf{q}|/\Lambda)$, with e.g. \mathcal{F} belonging to the function space $\mathcal{L}^2(\mathbf{R})$, (ii) compute the logarithmic derivatives with respect to the cutoff Λ of the fermion self-energy and vertices, (iii) identify the appropriate coefficients of the Taylor expansion (in k_i and ω_n) of the result. The choice of a soft cutoff is fairly arbitrary, but helps to avoid spurious singularities induced by “ringing” at the spectral edge. The derivative with respect to Λ serves to extract the *incremental* change in the band parameters due to a small change of cutoff, as in the Wilsonian view of RG. The momentum and frequency expansion allows identification of the renormalization of each term of the Hamiltonian independently.

A. Diagram expressions

The fermion self-energy is

$$\Sigma_f(\omega_n, \mathbf{k}) = \sum_{b=\varphi, \phi} \frac{-g_b^2}{N} \times \int \frac{d^3 q}{(2\pi)^3} \int_{-\infty}^{+\infty} \frac{d\Omega_n}{(2\pi)} \frac{M_b G_{\Omega_n, \mathbf{q}}^0 M_b \mathcal{F}\left(\frac{|\mathbf{q}|}{\Lambda}\right) \mathcal{F}\left(\frac{|\mathbf{k}-\mathbf{q}|}{\Lambda}\right)}{\Sigma_b(\omega_n - \Omega_n, \mathbf{k} - \mathbf{q}) - \Sigma_b(0, \mathbf{0})}, \quad (28)$$

where two cutoff functions \mathcal{F} are present because both fermion lines in the self-energy should be cutoff, i.e. the momenta of all the electrons in the theory are taken within the cutoff. Similarly, the vertex corrections *at zero external momenta and frequencies* are $\Xi_b^0 = \Xi_{b;(1)}^0 + \Xi_{b;(2)}^0$, with

$$\Xi_{b;(1)}^0 = \sum_{b'=\varphi, \phi} \frac{g_b g_{b'}^2}{N^{3/2}} \times \int \frac{d^3 q}{(2\pi)^3} \int_{-\infty}^{+\infty} \frac{d\Omega_n}{2\pi} \frac{M_{b'} G_{\Omega_n, \mathbf{q}}^0 M_b G_{\Omega_n, \mathbf{q}}^0 M_{b'} \mathcal{F}^2\left(\frac{|\mathbf{q}|}{\Lambda}\right)}{\Sigma_{b'}(\Omega_n, \mathbf{q}) - \Sigma_{b'}(0, \mathbf{0})}, \quad (29)$$

and

$$\Xi_{b;(2)}^0 = - \sum_{b', b''=\varphi, \phi; \eta=\pm} \frac{g_b g_{b'}^2 g_{b''}^2}{N^{5/2}} \int \frac{d^3 q_1}{(2\pi)^3} \int \frac{d^3 q_2}{(2\pi)^3} \int_{-\infty}^{+\infty} \frac{d\Omega_{n,1}}{2\pi} \int_{-\infty}^{+\infty} \frac{d\Omega_{n,2}}{2\pi} \times \frac{M_{b'} G_{\Omega_{n,2}, \mathbf{q}_2}^0 M_{b''} \text{Tr} \left\{ G_{\Omega_{n,1}, \mathbf{q}_1}^0 M_{b'} G_{\Omega_{n,1} + \eta \Omega_{n,2}, \mathbf{q}_1 + \eta \mathbf{q}_2}^0 M_{b''} G_{\Omega_{n,1}, \mathbf{q}_1}^0 M_b \right\}}{[\Sigma_{b'}(\Omega_{n,2}, \mathbf{q}_2) - \Sigma_{b'}(0, \mathbf{0})] [\Sigma_{b''}(\Omega_{n,2}, \mathbf{q}_2) - \Sigma_{b''}(0, \mathbf{0})]} \mathcal{F}\left(\frac{|\mathbf{q}_1|}{\Lambda}\right) \mathcal{F}\left(\frac{|\mathbf{q}_2|}{\Lambda}\right) \mathcal{F}\left(\frac{|\mathbf{q}_1 + \eta \mathbf{q}_2|}{\Lambda}\right). \quad (30)$$

All other diagrams are smaller in a $1/N$ expansion. By using for example $\partial_{-i\alpha\omega_n} G_{\omega_n, \mathbf{k}}^0 = -(G_{\omega_n, \mathbf{k}}^0)^2$, one can show that the two-loop diagrams, $\Xi_{b;(2);b',b'',\eta}^0$, with identical internal boson propagators ($b' = b''$) cancel out one another upon performing the sum over $\eta = \pm 1$ (and even vanish identically in the case $b = \phi$). The remaining two-loop diagrams correcting the Coulomb vertex ($b = \varphi$ and $b' \neq b''$) can also be shown to vanish, for example by noticing that only the $b' = b''$ diagrams can renormalize g . Therefore, only four two loop diagrams (those with $b = \phi$ and $b' \neq b''$), shown in Fig. 3 of the main text, need be calculated. Careful observation shows all contributions are equal, and an explicit calculation yields a finite integral, which converges to a nonzero value multiplied by $g/(N^{3/2} |\ln c_1/c_2|^2)$. This is actually subdominant (for $c_1/c_2 \ll 1$) to the contribution from the one loop vertex correction, although it is of the same order in $1/N$.

B. Flow equations

We find the following RG flow equations (“beta-functions”). The flow of α , the coefficient of the frequency in the fermion self-energy, is

$$\frac{\partial_\ell \alpha}{\alpha} = 3 - 2\Delta_\psi + \frac{1}{\alpha} (\partial_{-i\omega_n} [D_\Lambda \Sigma_f^0])|_{\omega_n=0, \mathbf{k}=\mathbf{0}}. \quad (31)$$

where $D_\Lambda = \Lambda \frac{d}{d\Lambda}$. As usual, the last term of the right-hand-side corresponds in the RG procedure to the “rescaling” (or integration of momenta), while the other terms correspond to the “renormalization” [31]. The “anisotropic” coupling of the fermions to the bosons leads to “anisotropic” corrections to the coefficients of the fermion Hamiltonian:

$$\frac{\partial_\ell c_j}{c_j} = z + 1 - 2\Delta_\psi + \frac{(\delta \Sigma_f)_j^0}{c_j}, \quad j = 0, 1, 2, \quad (32)$$

where

$$(\delta \Sigma_f)_j^0 = \begin{cases} \frac{1}{2} \left(\partial_{k_x, k_x}^2 [D_\Lambda \Sigma_f^0] \right) \Big|_{\omega_n=0, \mathbf{k}=\mathbf{0}} & \text{for } j = 0 \\ \sqrt{2} \left(\partial_{k_x, k_y}^2 [D_\Lambda \Sigma_f^1] \right) \Big|_{\omega_n=0, \mathbf{k}=\mathbf{0}} & \text{for } j = 1 \\ \sqrt{2} \left(\partial_{k_x, k_x}^2 [D_\Lambda \Sigma_f^4] \right) \Big|_{\omega_n=0, \mathbf{k}=\mathbf{0}} & \text{for } j = 2 \end{cases} \quad (33)$$

The RG equations for the coupling constants are simply:

$$\frac{\partial_\ell g_b}{g_b} = z + 3 - \Delta_\phi - 2\Delta_\psi + M_b^{-1} \frac{[D_\Lambda \Xi_b^0]}{g_b/\sqrt{N}}, \quad (34)$$

for $g_\phi = g, g_\varphi = ie$ and $M_\phi = \Gamma_{45}, M_\varphi = I$. The right-hand-sides of the equations eventually involve angular integrals that can be performed numerically, and which are obtained using the identities:

$$\begin{cases} \int_0^\infty dq \frac{1}{q} \Lambda \frac{d}{d\Lambda} [\mathcal{F}^2(q/\Lambda)] = 1 \\ \int_0^\infty dq \Lambda \frac{d}{d\Lambda} \left[\frac{\mathcal{F}(q/\Lambda) \mathcal{F}'(q/\Lambda)}{\Lambda} \right] = 0 \\ \int_0^\infty dq q \Lambda \frac{d}{d\Lambda} \left[\frac{\mathcal{F}(q/\Lambda) \mathcal{F}''(q/\Lambda)}{\Lambda^2} \right] = 0 \\ \int_0^\infty dq q_1 \frac{\Lambda}{q_1} \frac{d}{d\Lambda} [\mathcal{F}(q_1/\Lambda) \mathcal{F}(q_1 \tilde{q}_2/\Lambda) \mathcal{F}(q_1(1 + \tilde{q}_2)/\Lambda)] = 1 \end{cases} \quad (35)$$

(for any \tilde{q}_2), since $\mathcal{F}(0) = 1$ and $\mathcal{F}(+\infty) = 0$.

In practice, to calculate the flows of α and c_0 , from Eqs. (31) and (32) with $j = 0$, we shift the internal momentum in the integrands of Σ_f (see Eq. (28)), i.e. $\mathbf{q} \rightarrow \mathbf{q} + \mathbf{k}$. As a result, the derivatives with respect to the frequency ω_n or momenta k_i involve the fermionic part of the integrands. Proceeding otherwise to obtain the equation for c_0 leads to a divergent integral. For the flow of c_2 , where the derivatives with respect to either part of the integral converge, we have checked that both “methods” give the same result. The integrals from the vertex corrections converge, in particular, we find the double integrals in $[D_\Lambda \Xi_{b;(2)}^0]$ are subdominant (equal to a finite number times $1/|\ln c_1/c_2|^2$, the latter factor coming solely from the two inverse boson propagators), even upon taking $c_{0,1} = 0$ directly in G^0 .

C. Details of the flows of c_1 and c_2

Because the results are crucial to the physics, we give the details of the calculation of the beta functions for c_1 and c_2 . Applying the derivatives in Eq. (33) with $j = 1, 2$ to the “boson parts” of the integrand in the self-energies using the approximations discussed in Sec. II, and expanding Σ_b^{-1} in small $1/|\ln c_1/c_2|$, we find:

$$\frac{(\delta \Sigma_f)_1^0}{c_1} = -\frac{\sqrt{2}}{8\pi |\ln c_1/c_2| N} \int \frac{d\hat{\mathbf{q}}}{(2\pi)^2} \frac{d_1(\hat{\mathbf{q}})}{E_{\hat{\mathbf{q}}}} \left\{ (m_1^\varphi + m_1^\phi) \mathcal{N}_{1,1} + (m_2^\varphi + m_2^\phi) \mathcal{N}_{1,2} + (m_3^\varphi + m_3^\phi) \mathcal{N}_{1,3} \right\} \quad (36)$$

$$\frac{(\delta \Sigma_f)_2^0}{c_2} = -\frac{\sqrt{2}}{8\pi |\ln c_1/c_2| N} \int \frac{d\hat{\mathbf{q}}}{(2\pi)^2} \frac{d_4(\hat{\mathbf{q}})}{E_{\hat{\mathbf{q}}}} \left\{ (m_1^\varphi - m_1^\phi) \mathcal{N}_{2,1} + (m_2^\varphi - m_2^\phi) \mathcal{N}_{2,2} + (m_3^\varphi - m_3^\phi) \mathcal{N}_{2,3} \right\}, \quad (37)$$

where

$$\mathcal{N}_{1,1} = 3\hat{q}_x\hat{q}_y \quad (38)$$

$$\mathcal{N}_{1,2} = 5\hat{q}_x\hat{q}_y (-8\hat{q}_x^2\hat{q}_y^2 - 4\hat{q}_x^2\hat{q}_z^2 - 4\hat{q}_y^2\hat{q}_z^2 + 3\hat{q}_x^4 + 3\hat{q}_y^4 + 7\hat{q}_z^4) \quad (39)$$

$$\mathcal{N}_{1,3} = -\hat{q}_x\hat{q}_y\hat{q}_z^2 (6\hat{q}_x^2\hat{q}_y^2 - 43\hat{q}_x^2\hat{q}_y^2 + 6\hat{q}_y^2\hat{q}_z^2 + 10\hat{q}_x^4 + 10\hat{q}_y^4 - 4\hat{q}_z^4) \quad (40)$$

$$\mathcal{N}_{2,1} = 2\hat{q}_x^2 - \hat{q}_y^2 - \hat{q}_z^2 \quad (41)$$

$$\mathcal{N}_{2,2} = 24\hat{q}_x^2\hat{q}_y^2\hat{q}_z^2 - 21\hat{q}_x^4(\hat{q}_y^2 + \hat{q}_z^2) + \hat{q}_y^4(42\hat{q}_x^2 - 5\hat{q}_z^2) + \hat{q}_z^4(42\hat{q}_x^2 - 5\hat{q}_y^2) + 2\hat{q}_x^6 - 5\hat{q}_y^6 - 5\hat{q}_z^6 \quad (42)$$

$$\mathcal{N}_{2,3} = \hat{q}_y^2\hat{q}_z^2 (-31\hat{q}_x^2\hat{q}_y^2 - 31\hat{q}_x^2\hat{q}_z^2 + 4\hat{q}_y^2\hat{q}_z^2 + 30\hat{q}_x^4 + 2\hat{q}_y^4 + 2\hat{q}_z^4). \quad (43)$$

The relative signs of the terms coming from Σ_ϕ originate from the “opposite” commutation relations of $\Gamma_{1,2,3}$ and $\Gamma_{4,5}$ with Γ_{45} , i.e. $[\Gamma_a, \Gamma_{45}] = 0$ for $a = 1, 2, 3$ and $\{\Gamma_a, \Gamma_{45}\} = 0$ for $a = 4, 5$. Note that this is true before implementing any approximation or assumption on the magnitude of c_1/c_2 . If $e = 0$, it is then obvious that the flows of c_1 and c_2 will take different directions, i.e. that the ratio c_1/c_2 will be either relevant or irrelevant, or in other words, will flow either to infinity or zero. Hence a calculation taking c_1/c_2 large or small from the beginning is for sure valid. We find that $c_1/c_2 \rightarrow 0$ occurs for $e = 0$ (see below). When $e \neq 0$, the situation is not as clear-cut, but taking c_1/c_2 small, as when $e = 0$, proves to be self-consistent as shown below. We can also justify it *a posteriori* as follows. $c_1/c_2 \rightarrow +\infty$ would lead to a situation where the coupling term $\phi\psi^\dagger\Gamma_{45}\psi$ commutes with the bare Hamiltonian at the critical point, hence *removing* all fluctuations due to the coupling to the order parameter, which is supposed to drive the transition through the fluctuations it induces. Such a choice seems therefore unreasonable. The situation where $c_1/c_2 \rightarrow c^*$, a fixed constant, although perhaps seemingly more reasonable, would imply the existence of a universal ratio, when none seems to be natural. Hence, the limit $c_1/c_2 \rightarrow 0$ seems to be the only reasonable limit to be taken. $c_0/c_1 \rightarrow 0$ is also consistent.

D. Exponents

Keeping α, c_2, g and e constant, i.e. setting the corresponding flow equations to zero, the dynamical critical exponent and the field dimensions are

$$\begin{aligned} z &= 2 - \frac{a_z}{N|\ln c_1/c_2|}, & \Delta_\psi &= \frac{3}{2} + \frac{a_\psi}{N|\ln c_1/c_2|}, \\ \Delta_\phi &= \frac{3}{2} + \left[\frac{1}{2} + \frac{a_\phi}{N|\ln c_1/c_2|} \right], \\ \Delta_\varphi &= \frac{3}{2} + \left[\frac{1}{2} - \frac{a_\varphi}{N|\ln c_1/c_2|} \right], \end{aligned} \quad (44)$$

where $a_z = 0.063$, $a_\psi = 0.143$, $a_\phi = 0.255$, and $a_\varphi = 0.063$. The anomalous dimensions are then simply $\delta z =$

$a_z/(N|\ln c_1/c_2|)$, $\eta_\psi = 2a_\psi/(N|\ln c_1/c_2|^2)$, $\eta_\phi = 1 + 2a_\phi/(N|\ln c_1/c_2|)$ and $\eta_\varphi = 1 - 2a_\varphi/(N|\ln c_1/c_2|)$, as given in the main text.

E. Solutions to the flow equations

Finally, we obtain

$$\partial_\ell \left(\frac{c_1}{c_2} \right) = -\frac{c_1}{c_2} \frac{Y}{N|\ln c_1/c_2|}, \quad (45)$$

$$\partial_\ell \left(\frac{c_0}{c_1} \right) = -\frac{c_0}{c_1} \frac{W}{N|\ln c_1/c_2|}, \quad (46)$$

with $Y = 0.020$ and $W = 0.043$. These equations are solved analytically by

$$(c_1/c_2)(\ell) = e^{-\frac{v_0}{\sqrt{N}}\sqrt{\ell+\ell_0}}, \quad (c_0/c_1)(\ell) = \Upsilon_0 e^{-\frac{v'_0}{\sqrt{N}}\sqrt{\ell+\ell_0}}, \quad (47)$$

where $v_0 = \sqrt{2Y}$ and $v'_0 = \sqrt{2W}/\sqrt{Y}$, and where ℓ_0 and Υ_0 are constants which depend on $c_{0,1,2}(\ell = 0)$.

Note that, as mentioned in the main text, *in the absence of Coulomb interactions*, we find $(c_1/c_2)(\ell) = e^{-\frac{0.359}{\sqrt{N}}\sqrt{\ell+\ell_1}}$ and $(c_0/c_1)(\ell) \propto e^{\frac{0.240}{\sqrt{N}}\sqrt{\ell+\ell_1}}$ (ℓ_1 is a constant), i.e. c_0/c_1 is found to be a *relevant* parameter in that case. The latter means that, eventually, c_0 reaches $c_1/\sqrt{6}$, point at which Fermi surfaces start to develop, rendering our theory invalid and the heretofore studied critical point unstable. This would correspond to a Lifshitz transition.

IV. PHYSICAL QUANTITIES

We are now in a position to calculate the behavior of some physical quantities. We first extract the critical exponent of the correlation length. The associated RG flow is

$$\frac{\partial_\ell r}{r} = z + 3 - 2\Delta_\phi, \quad \text{i.e.} \quad \partial_\ell r = \nu^{-1}(\ell)r, \quad (48)$$

with

$$\nu^{-1}(\ell) = 1 - \frac{2a_\phi + a_z}{N|\ln c_1/c_2|}. \quad (49)$$

So

$$\partial_\ell r = \left(1 - \frac{A}{\sqrt{N}\sqrt{\ell+\ell_0}} \right) r, \quad \text{with} \quad A = \frac{2a_\phi + a_z}{v_0}, \quad (50)$$

i.e. $A = 2.836$, which is solved into

$$r(\ell) = r_0 e^{\frac{\ell - \frac{2A}{\sqrt{N}}\sqrt{\ell+\ell_0}}{\nu^{-1}(\ell)}}, \quad (51)$$

where r_0 is a constant which depends on $r(\ell = 0)$. We can easily invert $r = r(\ell)$ to $\ell = \ell(r)$ by taking the log of

Eq. (51), squaring both sides and solving the quadratic equation. We get:

$$\ell \approx \ln \frac{r}{r_0} + \frac{2A}{\sqrt{N}} \sqrt{\ln \frac{r}{r_0} + \ell_0}, \quad (52)$$

where we have kept only terms to order $1/\sqrt{N}$.

A. Order parameter exponent

We first extract the exponent β and its logarithmic correction, i.e. how $\langle \phi \rangle$ behaves with r . We write

$$\frac{\phi(\ell + d\ell) - \phi(\ell)}{\phi(\ell + d\ell)} \approx d\ell \Delta_\phi(\ell), \quad (53)$$

and integrate both sides from 0 to ℓ . Using Eq. (52), we obtain

$$\begin{aligned} \frac{\phi}{\phi_0} \sim \left(\frac{r}{r_0} \right)^2 \exp \left[2 \frac{5a_\phi + 2a_z}{v_0 \sqrt{N}} \sqrt{\ln \frac{r}{r_0} + \ell_0} \right] \\ \times \exp \left[\frac{-2a_\phi \sqrt{\ell_0}}{v_0 \sqrt{N}} \right], \end{aligned} \quad (54)$$

with $2 \frac{5a_\phi + 2a_z}{v_0} = 13.867$ and $2a_\phi/v_0 = 2.523$ (in the main text, we absorbed ℓ_0 in the definition of r_0). Contrary to more conventional problems, like the usual Ising model, where $\beta_{\text{Ising}} = 1/2$ in three spatial dimensions, the bosonic order parameter here grows very slowly as one moves away from the critical point on the ordered side of the transition. This can be seen to be due to the massive fluctuations of the boson field due to the strong coupling to the fermions.

B. Specific heat

At the critical point (or in the quantum critical region), temperature is the only relevant parameter, so thermal properties receive intriguing corrections in our critical theory. Since the fermion is well-defined ($\eta_\psi \rightarrow 0$), the thermal average of the energy is

$$\langle E \rangle = \sum_{i=\pm, \mathbf{k}} \langle n_{i, \mathbf{k}} \rangle E_i(\mathbf{k}) = \sum_{i, \mathbf{k}} \frac{2}{e^{\beta E_i(\mathbf{k})} + 1} E_i(\mathbf{k}), \quad (55)$$

with, for $\langle \phi \rangle = 0$, $c_0 = 0$ and $c_2 = 1$, $E_\pm(\mathbf{k}) = \pm \frac{\mathbf{k}^2}{\sqrt{6}} \sqrt{1 + 3(c_1^2 - 1)w_{\mathbf{k}}^2}$ where $w_{\mathbf{k}} = \hat{k}_x^2 \hat{k}_y^2 + \hat{k}_x^2 \hat{k}_z^2 + \hat{k}_y^2 \hat{k}_z^2$. To lowest order, we find

$$\begin{aligned} C_V = \partial_T \langle E \rangle &\approx \frac{15(4 - \sqrt{2})6^{3/4}\sqrt{\pi}}{16} \zeta(5/2) \frac{T^{3/2}}{c_1^{3/2}} \\ &\approx 22.1 \exp \left[\frac{3v_0}{2\sqrt{N}\sqrt{z}} \sqrt{\ln \frac{T_0}{T}} \right] T^{3/2}, \end{aligned} \quad (56)$$

where $3v_0/(2\sqrt{z}) \approx 0.215$ (we use $z \approx 2$). To obtain the last line, we used the approximation $e^\ell = (T(\ell)/T_0)^{1/z}$

and thereby solved the RG equation of c_1 in terms of temperature. The logarithmic correction to the $T^{3/2}$ law is a signature of the fact that c_1 becomes scale (temperature)-dependent in the quantum critical region.

V. MEAN-FIELD THEORY

In this section we consider the behavior in the ordered phase according to naïve mean field theory, i.e. a saddle-point evaluation of the φ and ϕ integrals. The former saddle point is simply $\varphi = 0$, i.e. there are no effects of the long-range Coulomb interactions at the mean field level. The saddle point value of ϕ is non-zero in the antiferromagnetic phase. It is governed by the effective action which consists of the bare one (second line of Eq. (1) of the main text) *plus* the contribution obtained by integrating out the fermions.

The fermionic contribution to the effective action, for constant ϕ , is simply the space-time integral of the total ground state energy density of the electrons. This is obtained by summing up the energy of occupied single-particle states.

In the saddle point approximation, the Hamiltonian density of the fermions is

$$\mathcal{H}_{\text{MF}}^\psi[\phi] = c_0 \mathbf{k}^2 + \sum_{a=1}^5 \hat{c}_a d_a(\mathbf{k}) \Gamma_a + \phi \Gamma_{45}, \quad (57)$$

and we therefore have the ground state energy density

$$\mathcal{E}_{\text{MF}}^\psi[\phi] = \sum_{\alpha=1}^2 \int_{\Lambda} \frac{d^3 k}{(2\pi)^3} E_{\mathbf{k}}^\alpha[\phi], \quad (58)$$

($E_{\mathbf{k}}^{1,2}$ are the single-particle lowest-energy bands, with $E_{\mathbf{k}}^{1,2}[\phi = 0] = E_{\pm}(\mathbf{k})$). Here, by diagonalizing $\mathcal{H}_{\text{MF}}^\psi[\phi]$, we obtain

$$\begin{aligned} E_{\mathbf{k}}^{1,2,3,4}[\phi] &= c_0 \mathbf{k}^2 \\ &\pm \frac{1}{\sqrt{6}} \sqrt{c_2^2 \mathbf{k}^4 + 2(c_1^2 - c_2^2)w_{\mathbf{k}}^2 \mathbf{k}^4 \pm 6\sqrt{2}c_1 \mathbf{k}^2 w_{\mathbf{k}} \phi + 6\phi^2}, \end{aligned} \quad (59)$$

where we define $\mathbf{k}^4 = (\mathbf{k}^2)^2$, and where 1, 2, 3, 4 correspond to the signs $\{-, -, -, +, -, +, +\}$, respectively.

From scaling, $E_{\mathbf{k}}^{1,2} \sim \mathbf{k}^2$, and hence, from Eq. (58), one expects that the singular scaling contributions to the effective action behave as $\mathcal{E}_{\text{MF}}^\psi \sim |\mathbf{k}|^5 \sim |\phi|^{5/2}$, where we used $\phi \sim \mathbf{k}^2$, which follows dimensionally from $\mathcal{H}_{\text{MF}}^\psi$. This describes only the singular contributions. Since $\mathcal{E}_{\text{MF}}^\psi$ is an even function of ϕ , we expect it to contain constant and quadratic terms as well (which are cutoff-dependent). Indeed one can verify by direct expansion in ϕ that the integrals which arise from Eq. (58) as coefficients of unity and ϕ^2 are finite, but if one proceeds to the following order, the coefficient of ϕ^4 is divergent. This is due to the presence of the $t|\phi|^{5/2}$ term.

To extract the coefficient t , we take three derivatives of $\mathcal{E}_{\text{MF}}^\psi[\phi]$ with respect to ϕ . We find an integral whose integrand goes as $1/|\mathbf{k}|^6$ at large $|\mathbf{k}|$, so that the result is integrable in that region. One then simply rescales $\mathbf{k} \rightarrow \mathbf{k}/\sqrt{|\phi|}$, and takes the limit of small ϕ (i.e. $\Lambda/\sqrt{\phi} \rightarrow +\infty$). This makes the singular behavior explicit, and in this limit we find $\partial_{\phi,\phi,\phi}^3 \mathcal{E}_{\text{MF}}^\psi[\phi] = 1.079/\sqrt{\phi}$, i.e. $t = 1.079 \times \frac{8}{15} = 0.575$, where the coefficient was determined by a numerical integration taking the fixed-point values $c_0 = c_1 = 0$. Therefore, $t|\phi|^{5/2}$ is indeed the lowest-order nonanalytical term. Hence, putting everything together, and looking at the boson action with the

fermions integrated out, we have:

$$\mathcal{S}_{\text{MF}}[\phi] = V \int d\tau \left[r\phi^2 + \mathcal{E}_{\text{MF}}^\psi[\phi] \right] \quad (60)$$

$$\sim V \int d\tau \left[r'\phi^2 + t|\phi|^{5/2} \right], \quad (61)$$

all other terms being irrelevant. Above, r' includes the ϕ^2 terms in $\mathcal{E}_{\text{MF}}^\psi[\phi]$. Most importantly, we obtained positive $t > 0$, so that when $r' < 0$, a stable minimum action configuration exists, describing a continuous –but unconventional– transition at the mean field level.